D101

The height limit and earth pressure characteristics of benched slope in centrifugal model tests

〇Shanzhi TAO, Thirapong PIPATPONGSA

1. Introduction

With the capability in decreasing the overall gradient of a slope, the slope benching technique is an alternative to additional supporting structures. This method has been used widely for its cost-efficiency. This study presents a design scheme for the benched slope by following a 2D plane sliding surface assumption suggested by Francais and Culmann [1, 2]. Centrifuge tests with different model dimensions were conducted. The recorded data of earth pressure in the benched slope was employed to evaluate the shear strength reduction ratio r_d for lateral confinement. The failure moments were also compared with the theoretical prediction.

2. Basic theory

2.1 The limit height of a benched slope

The assumed force diagram of the potential wedge-shaped sliding block is shown in Fig. 1 in 2D condition where β is the angle of the slope, α is the potential failure plane, F_D is the driving force and S_α is the resisting force based on the Mohr-Coulomb failure criterion.

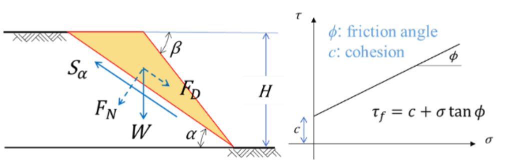

Fig. 1 The force diagram of a sliding block and the Mohr–Coulomb failure criterion

The factor of stability (FS) can be defined by Eq. (1), where ρ_t is the wet density, c is the cohesion and ϕ is the internal friction angle of soil. Minimizing FS with respect to α through Eq. (2) lead to the critical failure plane, indicating that α is the half of the sum between β and ϕ.

$$FS = \frac{S_\alpha}{F_D} = \frac{2c}{\rho_t g H (sin\alpha)^2 (cot\alpha - cot\beta)} + \frac{tan\phi}{tan\alpha} \quad (1)$$

$$\frac{\partial FS}{\partial \alpha} = 0,\ \alpha = \frac{\beta + \phi}{2} \quad (2)$$

Substituting of Eq. (2) into Eq. (1), FS can be achieved. The height limit of the bare slope is thus obtained as Eq. (3) by assigning FS=1 in Eq. (1).

$$H = \frac{2c}{\rho_t g\,(sin\,\alpha)^2 (cot\alpha - cot\beta)(1 - \frac{tan\phi}{tan\alpha})} \quad (3)$$

In Fig. 2, there is a parallelogram-shaped bench on the slope toe. If the additional resistance force ΔS_α provided by the weight of a bench is enough to protect the slope from sliding along O_1A_1, the position of the critical failure plane would change to O_2A_2. If the exposed part could stay stable either, the total slope would be safe. Finally, the limit height of the benched slope can be determined by Eq. (4).

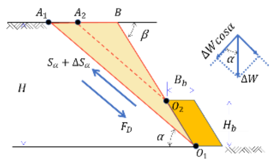

Fig. 2 The force diagram of the benched slope

$$H = \frac{2c}{\rho_t g\,(sin\,\alpha)^2 (cot\alpha - cot\beta)(1 - \frac{tan\phi}{tan\alpha})} + H_b \quad (4)$$

2.2 Shear strength reduction ratio r_d

Concerning the shear strength reduction technique [3, 4]. The intermediate state between passive and active can be expressed by using shear strength reduction ratio r_d described in Eq. (5) where σ'_h and σ'_v denote the effective horizontal stress and vertical stress, respectively.

$$r_d = \frac{\sigma'_h - \sigma'_v}{2\sqrt{(\sigma'_v tan\phi + c)(\sigma'_h tan\phi + c)}} \quad (5)$$

3. Test program

3.1 The property of the material

Only the details about one of case 7 are focused here. The material used in this study is Hiroshima sand for which c=4.1 kPa, ϕ=35.5° was obtained from direct shear tests to obtain the peak strength with a water content of 8% under a compaction degree of 80%.

3.2 The initial conditions of experiments

The diagram and configuration of gauges in this case are shown in Fig. 3. There was a bench on the toe of the left slope having a height of 7.5 cm and a width of 3 cm, the same breath as the slope of 40 cm in model scale.

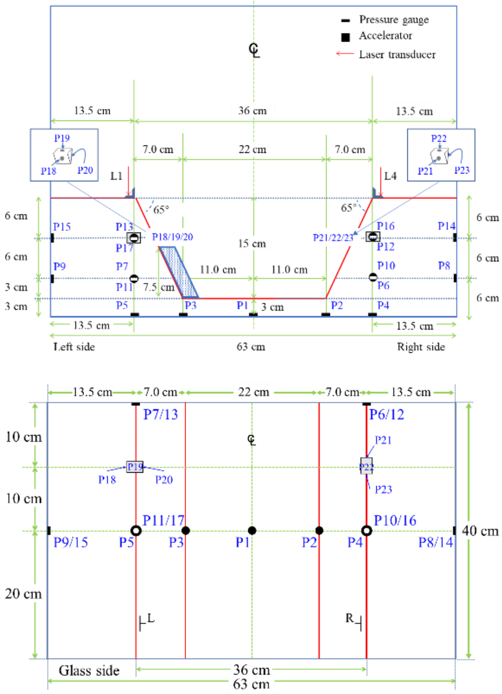

Fig. 3 Front and top view of case 7

3.3 Experimental process

The model was accelerated to 50g first. Then, the acceleration was increased by 10g increment.

4 Results

The test results of case 7 are shown in Fig. 4.

(1) The vertical dash line is the predicted centrifugal acceleration of the failure. The vertical arrows denote the centrifugal acceleration when the failures happened in the experiment. For the left side, the failure did not occur until 89g. For the right side, the first local toe failure happened at 27.8g, then several local failures continue after it. Under 47.1g, the local failure expanded to a toe failure across the crest. The predictions are comparable to the experimental results.

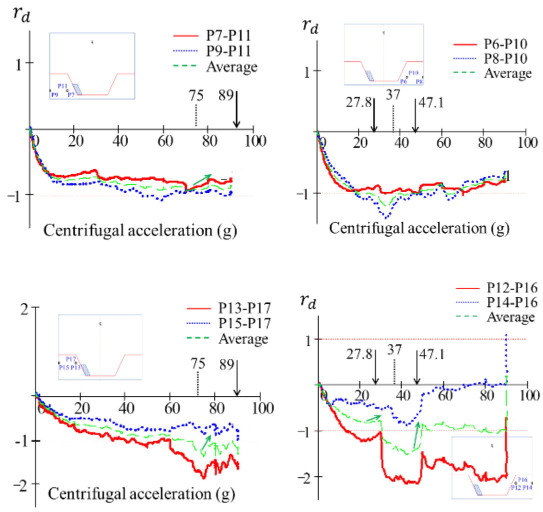

Fig. 4 Comparison between prediction and experimental results

(2) The other three lines in each figure imply the r_d changes with respect to the centrifugal acceleration before the peak value. In each position, r_d is evaluated from two sets of earth pressure sensors. It shows that similar trends are reflected. The values of r_d decrease inside the active state (<0) with increasing centrifugal acceleration, namely, the height of the slope in prototype scale. Around the real failure time, the r_d would bounce upwards. Because of the existence of boundaries, the slope did not deform uniformly even at the same height. When the average value is smaller than the limit active states -1, it is beyond the possible state and failure happened. Then, their values return to the limit active states.

Reference

1) Francais, *Recherches sur la poussee des terres sur la forme et les dimensions des murs de revetment et sur les talus d'excavation*. 1820: Paris.

2) Culmann, C., *Graphische statik.* Zurich, 1866.

3) Dawson, E.M., W.H. Roth, and A. Drescher, *Slope stability analysis by strength reduction.* Géotechnique, 1999. **49**(6): p. 835–840.

4) Pipatpongsa, T., et al., *Stability analysis of laterally confined slope lying on inclined bedding plane.* Landslides, 2022. **19**(8): p. 1861-1879.